Supporting Information

Bernal et al. 10.1073/pnas.1121448109

SI Methods

Hubbard Brook Experimental Forest Historical Datasets and Statistical Analysis. We analyzed hydrometeorological and historical chemistry data as well as forest inventories from the Hubbard Brook Experimental Forest (HBEF) for watershed 6 (W6)—the biogeochemical reference watershed at HBEF (43°56′ N, 71°45′ W). These data are available at http://www.hubbardbrook.org/ (unless otherwise specified in the text).

Atmospheric N deposition and stream water nitrate data. We calculated monthly bulk inorganic N (NO_3^--N and NH_4^+-N) deposition at W6 since 1963 by multiplying monthly precipitation by volume weighted average (VWA) monthly concentration for bulk precipitation. We estimated the relative contribution of dry atmospheric N inputs to bulk N precipitation using wet and dry N deposition data recorded by the Clean Air Status and Trends Network (http://www.epa.gov/CASTNET/) for locations nearby the HBEF area since 1989 (WST109 station). Atmospheric input of dissolved organic nitrogen was measured since 1995 (1). We calculated VWA monthly stream water nitrate loads at W6 since 1963 by multiplying monthly stream discharge by VWA monthly nitrate concentration recorded at the W6 stream gauging station.

Stream flow and precipitation measurements as well as accuracy of chemical analysis have varied little since the beginning of the HBEF records (2, 3). However, quantification of N fluxes is subjected to uncertainties inherent to both water flow measurement and analytical precision. These uncertainties are additive, and they result in a 5–15% variation in estimates of annual N fluxes for both stream water and precipitation (2, 4, 5).

Global Inventory Modeling and Mapping Studies satellite data. We used the satellite-derived Global Inventory Modeling and Mapping Studies (GIMMS) dataset to assess changes on the length of the growing season over time. The GIMMS dataset is a normalized difference vegetation index (NDVI) available each 15 d since 1982. These data are obtained from the Advanced Very High Resolution Radiometer (AVHRR) onboard the National Oceanic and Atmospheric Administration satellite (http://www.landcover.org/data/gimms). We analyzed GIMMS NDVI values from a 10×10 km^2 cell centered on the HBEF area (43°57′ N, 71°45′ W) using $NDVI_{max}/2$ as a proxy of the start and the end of the plant growing season. The first day of the year (DOY), when $NDVI > NDVI_{max}/2$ (DOY_0), and the first DOY > 180, when $NDVI < NDVI_{max}/2$ (DOY_f), were considered the beginning and the end of the plant growing season, respectively. We calculated the length of the plant growing season as $DOY_f - DOY_0$ (6) for the period of 1982–2006.

Soil temperature data. We analyzed weekly soil temperature records provided by the US Forest Service. Data were recorded with Colman fiberglass sensors at different depths (8, 15, and 30 cm) located at 300 m southwest of the stream gauge for watershed 4 from 1961 to 1998 (2). We also analyzed weekly soil temperature data recorded since 2003 by means of encapsulated thermistors installed at the same location and at similar depths provided by the US Soil Climate and Analysis Network (SCAN) (http://www.wcc.nrcs.usda.gov/scan/).

For each soil depth, we estimated monthly average ± SD soil temperature, and we performed statistical tests to ensure no bias between the two different datasets. The existing period for SCAN soil temperature data (2003–2008) was compared against the initial and the final 6-y period recorded with Colman sensors (1961–1966 and 1993–1998, respectively). Monthly soil temperatures recorded during 1993–1998 (last 6 y of Colman data) and 2003–2008 (SCAN data) were not significantly different (Table S1). In all cases, soil temperature during these two periods was higher than during 1961–1966, albeit differences were not always significant (Table S1). Based on this intercomparison analysis, we concluded that there was no evidence of bias between records.

Forest inventory data. The HBEF forest inventory is one of the most complete US inventories to date (7–10). Starting in 1965 and occurring every 5 y after 1977, the inventory includes information about the health status and above- and belowground biomass for all trees ≥10 cm dbh in the HBEF watersheds. A subsample of trees ≥2 and <10 cm dbh is also measured each time.

We analyzed the censuses from 1965 to 2002 at W6 to quantify changes in total live tree biomass, and changes on the basal area of healthy trees [diameter at breast height (DBH) ≥10 cm] and saplings (2 cm ≤ dbh < 10 cm) of the two most common hardwood species in the HBEF area: sugar maple (*Acer saccharum*) and American beech (*Betula allegheniensis*). The 2007 total live tree biomass was as reported in the work by Lindenmayer and Likens (7).

Snow deposition and snowpack data. We used weekly snow depth data recorded since 1956 by the US Forest Service at the W6 snow course to assess the maximum snow depth (M) reached every winter season. We quantified the total amount of precipitation stored in the snowpack during every season (S) by summing up only the increases in snow depth recorded every week at the snow course. For a given year, we quantified the fraction of snow precipitation melted in intermittent warming events (f; rather than exiting the catchment in the spring snowmelt pulse; i.e., $1 - f$) with $1 - M/S$, and therefore, f approaches zero when almost no intermittent winter melt events occur.

We used weekly snow depth records at W6 to assess the beginning and the end of the snowpack period for every winter season. We estimated precipitation input of inorganic N during the snowpack period by multiplying VWA monthly concentration of bulk inorganic N deposition at W6 by monthly precipitation. Then, we placed an upper limit of the potential effect of increased soil microbial immobilization during snowmelt on reducing nitrate export at the HBEF by assuming that inorganic N in snowmelt bypassed soils during the high nitrate period of 1969–1976 but was fully intercepted and immobilized by soils since 1977.

Statistical analysis. We used linear regression to analyze annual long-term trends for climatic, hydrological, and chemical variables. We calculated the slope ± SE and the 95% confidence interval of the linear regression, and we tested each linear model with ANOVA. We also analyzed long-term trends by month for soil temperature and stream water nitrate (concentration and flux). Correlation between pairs of variables was determined by means of the Spearman's ρ coefficient. Differences between groups of variables were determined by means of the Wilcoxon rank sum test. Nonparametric analyses were chosen, because data were not assumed to be normally distributed (11).

Water Sample Collection During the 2008 Spring, Archived Samples, and Chemical Analysis. ***Spring sample collection.*** We collected daily stream water samples from W6 before, during, and after the 2008 spring pulse of snowmelt discharge (from March 18, 2008 to May 5, 2008; $n = 50$). Samples were kept at ambient temperature (on average <4 °C) and immediately frozen on arrival at the laboratory. Samples were thawed and filtered through prewashed GF/F filters before laboratory analysis. Bulk deposition and snow samples were collected on a monthly basis from March to May ($n = 5$ and $n = 3$, respectively). These samples were immediately filtered through prewashed GF/F filters and kept frozen until analyzed. The first

10-mL water sample was discarded each time, and only one GF/F filter per sample was used.

Archived samples. Stream water and bulk deposition samples from the different weirs and meteorological stations at HBEF have been stored at the US Department of Agriculture, Forest Service headquarters from as early as 1963. These archived samples had been kept at room temperature after adding reagent-grade chloroform for preservation (3) (1 mL L^{-1}). We had access to archived samples from 1982 to 2007 collected at the weir of W3 (the hydrological reference watershed at HBEF) and bulk deposition samples from the rain gauge station 1 (43°57′ N, 71°44′ W). The HBEF historical data indicate that stream nitrate loads at W3 and W6 had a similar trend over time (12), and we were confident that any pattern exhibited by stream water samples at W3 would resemble the pattern at W6. We selected a subset of 75 archived stream water samples to investigate whether the isotopic signal of nitrogen in nitrate ($\delta^{15}N\text{-}NO_3^-$) changed with stream water nitrate concentration. We also gleaned 25 archived bulk deposition samples to assess whether changes in the $\delta^{15}N\text{-}NO_3^-$ in stream water archived samples were caused by changes in the isotopic signature of atmospheric N input. Based on our preliminary results, we chose only archived samples from December to April (the dormant period) when warming was most rapid and drop in nitrate export was more remarkable over time.

Chemical analyses. All water samples were analyzed for nitrate with a Dionex ionic chromatograph, and the $\delta^{15}N\text{-}NO_3^-$ and $\delta^{18}O\text{-}NO_3^-$ isotopic signatures were analyzed using the denitrifier method (13, 14). To minimize the influence of any storage effects on the isotopic signature of nitrate, we considered only archived samples for which there was no evidence that nitrate levels had changed significantly since they were first measured. Our criterion was fulfilled only in 19 of 100 samples and comprised 11 stream water samples and 8 bulk deposition samples from winter and early spring (January to April) for the period of 1990–2007.

SI Results and Discussion

Local Effect of Global Climate Warming at the HBEF and Possible Links to Nitrate Decline. Temperature is a key factor controlling catchment water budgets and biological processes, and not surprisingly, climate warming is inducing significant changes in hydrological processes and biological activity in the northeastern United State and Europe (15–19). At the HBEF, for instance, historical records revealed local changes in climate and snow hydrology. First, there was a long-term increase in air temperature since 1955, most strongly during winter (20). Concordantly, growing degree days (the accumulation of °C > 4 °C in air temperature since the first of January) have increased by the end of March and April (March: $r^2 = 0.23$, slope = 0.53 ± 0.14 °C y^{-1}; April: $r^2 = 0.12$, slope = 0.93 ± 0.35 °C y^{-1}; in the two cases, $n = 52$ and $P < 0.02$). Annual mean stream water temperature has also increased since 1980 (0.038 °C y^{-1}) (21). Second, we found a long-term trend increase in monthly mean soil temperature (0.024–0.048 °C y^{-1}) since the 1960s, particularly during the dormant season (from December to March) (Table S2) when the soil at HBEF was covered by snow. Monthly mean soil temperatures, however, showed no trend in late spring and summer (from April to September; for all months, $P > 0.05$). Finally, the number of days when ice covers the Mirror Lake (located within the Hubbard Brook Valley) has declined at a rate of 0.5 d y^{-1} since 1968 (18). Previous examinations of the HBEF snow pack records indicated significant declines in snow depth and snow cover duration (20). We also analyzed such records in detail; we found that the period of snow cover has shortened by 6 ± 2 d decade^{-1} ($r^2 = 0.14$, $P < 0.01$, $n = 51$), and maximum snow depth has declined by 6 ± 2 cm decade^{-1} ($r^2 = 0.16$, $P < 0.01$, $n = 51$) since 1956 at W6. These findings indicate that the HBEF has experienced a substantial warming over the past five decades and more notably, that climate conditions from late fall to early spring are becoming more favorable for biological activity.

Historical records also raised the possibility of a significant link between climate and nitrate trends in the HBEF. First, stream nitrate concentration has declined most strongly during the December to April Period when concentrations are the highest (Fig. S1), coinciding with the period of most rapid soil warming. Analysis of the long-term trend of nitrate export by month also revealed the strongest decline in export during April (at a rate of 0.14 ± 0.03 kg N ha^{-1} y^{-1}, $r^2 = 0.38$, $P < 0.001$, $n = 45$); declines were significant but small in other months. We found a moderate negative correlation between soil temperature and stream water nitrate in winter, especially in December and March when not only stream water concentrations but also nitrate fluxes were related to soil temperature (Table S3). That stream water nitrate declines with increases in soil temperature suggests that more favorable climatic conditions over time could be inducing increased immobilization and/or removal of nitrate by biota during the nonvegetative period, which could be, at least, partially responsible for the decline in nitrate loss observed at HBEF in the last decades.

Effect of Changes in Species Composition on Soil N Immobilization and Leaching: A Modeling Approach. There is an increasing body of knowledge showing the interaction between forest species composition and soil nutrient cycling. Litter from sugar maple, for instance, tends to decompose faster than litter from other hardwood species, bringing about higher nitrification rates and lower C and C:N ratios in the forest floor (22–26). Forest disturbances, whether natural or human-induced, promoting species replacement in hardwood forests could, therefore, have a dramatic impact on the N cycling at the scale of the entire ecosystem.

In the HBEF, sugar maple is being replaced by American beech—a species with tissues that are more recalcitrant to decomposition (22). Forest censuses at HBEF revealed that the contribution of sugar maple to the total basal area of W6 has decreased by 26%, whereas American beech's contribution has increased by 29% since they were first measured in 1965. We investigated the possibility that such changes in species composition would modify N immobilization in the soil pool and N leaching over time by applying a simple mechanistic model (Fig. S2) based on first-order kinetics (27). We considered specific decomposition rates for sugar maple and beech leaf litter, the two most common hardwood species at the HBEF (together contributing to 40% of the total basal area of W6). To model solely the effect of changes in species composition, we considered a constant input of leaf litter to the forest floor pool over time. For a given year, the fraction of leaf litter for each tree species was equivalent to the fraction by which each of these species contributed to the total basal area of healthy trees in the low and mid-elevations (545–783 m above sea level) of the W6, where hardwood forest predominates (http://www.hubbardbrook.org/data). We approximated the forest floor dynamics with a single pool linear model for each species (Eq. **S1**):

$$\frac{dL_i}{dt} = f(t) - k_i L_i. \qquad \textbf{[S1]}$$

Where L is the amount of litter in the forest floor, k is the decomposition rate for each tree species i, and $f(t)$ is the input of leaf litter to the forest floor at each time step that is linearly interpolated between times of the census. The total amount of leaf litter entering the system was considered to be constant over time and equal to 3,117 kg of dry weight (DW) ha^{-1} y^{-1}, which is the average for the whole period from 1965 to 2002 (8) according to the Landscape Biomass Tool of the HBEF (http://www.hubbardbrook.org/w6_tour/biomass-stop/biomassw6.htm). We ran the model using the decomposition rates (k_i) reported for the HBEF (0.25 and 0.08 for sugar maple and American beech, respectively) (22). We assumed the steady state solution for litter inputs in year 1965 as initial condition for L_i.

In a first scenario, we assessed whether changes in the litter/soil organic matter stock caused by species shift were responsible for the decline in nitrate loss (that is, if slower decomposing litter of American beech has led to retention of nitrogen). We estimated the relevant nitrogen content in the litter/soil organic matter ($N_{L,i}$) complex with (Eq. **S2**)

$$N_{L,i}(t) = \frac{\rho L_i(t)}{r_i}, \qquad \textbf{[S2]}$$

where ρ denotes the amount of carbon per unit DW (0.4 kg kg^{-1}) and r_i is the C:N ratio of the specific litter type (23.7 and 22.0 for sugar maple and American beech, respectively; http://www.hubbardbrook.org/data). The C:N ratios were kept constant over time, because available data (1992–2003) do not show any consistent temporal pattern in C:N of leaf litter for these two tree species (http://www.hubbardbrook.org/data).

Our calculations support the common expectation that a higher proportion of American beech litter in the forest floor promotes N accumulation in the litter soil complex (Fig. S3*A*). According to our results, however, a shift from sugar maple to American beech, such as reported for HBEF, would imply an increase in soil N immobilization of only ∼3 kg N ha^{-1} in a 25-y period, an amount that does not explain the drop in nitrate export (Fig. S3*A*).

In subsequent scenarios, we tested whether the tendency to reduced sugar maple abundance can account for the decline of nitrate exports caused by reduced nitrification and N losses in the forest floor pool. At each time step, the amount of mineralized litter for each species (M_i) based on Eqs. **S1** and **S2** was given by (Eq. **S3**)

$$M_i(t) = k_i \frac{\rho L_i(t)}{r_i} = k_i N_{L,i}(t), \qquad \textbf{[S3]}$$

and we partitioned the mineralization flux into ammonium and nitrate using different mineralization to nitrification (M:N) ratios. In scenario 2, we considered empirical M:N ratios as a proxy of the NH_4^+-N:NO_3^--N ratios in the forest floor. For each tree species, we estimated a mean M:N ratio based on values reported in empirical studies from HBEF and locations nearby (24, 25) (1.7:1 and 3.4:1 for sugar maple and beech, respectively). As a simplification, we considered that all NO_3^--N is leached from the system and that all NH_4^+-N is retained. In scenario 3, we assessed how large the effect of a shift from high- to low-quality litter could be on the leaching of available N from the forest floor pool by assuming an M:N ratio of 1:1 (all available N is nitrified and consequently leached) for high-quality litter (sugar maple) and 1:0 (there is no nitrification) for low-quality litter (American beech). We acknowledge that such phenomenological nitrification rates are not expected to occur in nature, but they illustrate the upper limit of the impact that a species replacement of the nature and the magnitude recorded at the HBEF may have on the leaching of available N from the forest floor.

According to our model, a shift in tree species composition, such as reported at HBEF, would imply a drop of nitrate leaching from the forest floor of 5 kg N ha^{-1} 25 y^{-1} (scenario 2) to 19 kg N ha^{-1} 25 y^{-1} (scenario 3) (Fig. S3*B*). Our results suggest that changes in N immobilization and N leaching from the forest floor promoted by the shift in species composition reported at HBEF could contribute only moderately, from 4% to <16%, to decreased nitrate losses from W6.

Modeling the Long-Term Effect of Historical Perturbations on Forest N Dynamics. Although past disturbances can promote significant disruptions on ecosystem functioning at different temporal scales, the long-term impact of natural perturbations and land use history on N cycling remains elusive in many cases (28–30). In HBEF, harvesting was a common practice until the beginning of the 20th century. The W6 forest was harvested two times (in 1906 and 1917), and some tree mortality resulted from the 1938 hurricane and the 1998 ice storm in the W6 area (31–33). Although historical values of tree mortality are poorly known, estimates published in the literature (31) suggest that harvesting was light in 1906 (∼20%) and substantial in 1917 (∼60%). We explored, using the Princeton Geophysical Fluid Dynamic Laboratory LM3V land model, a dynamic vegetation model with prognostic C–N cycles (34), the effect of past events of tree mortality on soil N dynamics and nitrate leaching over time at HBEF. In LM3V, carbon and nitrogen in vegetation are allocated to five pools: leaves, roots, storage, sapwood, and wood. Photosynthesis and nitrogen intake are adjusted to maintain C:N ratios in the different pool, whereas the storage pool is used to (*i*) store retranslocated carbon before leaf senescence and (*ii*) buffer nitrogen in plants against seasonal asynchrony of productivity and nitrogen supply. A plant functional type-specific fraction of N is retranslocated before leaf senescence (34, 35). Litterfall is partitioned according to quality in a fast and slow litter pool, and decomposition of the slow litter pool is incomplete and results in formation of soil organic matter, with immobilization of N. Nitrogen exports include both organic and inorganic forms. Soil organic matter and plants have precedence for inorganic N forms over exports. The model is forced with a recurring climate, where the climate variables are recycled over a period of 16 y. The climate forcing (temperature, solar radiation, wind, surface pressure, and relative humidity) is based on 3-h reanalysis data (36) integrating observations over the years 1951–1966. LM3V was spun up from bare ground until equilibrium (negligible drifts in carbon and nitrogen pools) before entering the transient simulation with the disturbances.

We subjected the model to probable scenarios with a Monte Carlo approach considering different harvest intensities for the 1906 and 1917 events for which the severity of perturbation was more uncertain. We ran 500 scenarios with tree mortality ranging from 5% to 95% and vegetation removal after harvesting ranging from 50% to 90% for each of the two harvest events. Parameters were varied in 5% intervals, and Monte Carlo draws were based on a uniform distribution. In all scenarios, the mortality of trees because of the 1938 hurricane and the 1998 ice storm was 20% and 30% of the total live biomass, respectively (32, 33).

The model captured the general pattern of increasing nitrate losses that gradually returned to predisturbance conditions (Fig. S4*A*). This pattern was explained mainly by the disequilibrium between litter inputs and soil pools: a first phase of high N immobilization occurred because of harvest residuals or windthrow material and vegetation uptake; subsequent losses were caused by a decrease in the soil organic matter pool with litter inputs below the predisturbance value. A final phase was characterized by soil organic matter buildup as vegetation pools and litter input returned to the long-term steady state (Fig. S4 *B* and *C*). Model simulations suggest that it takes several centuries for the vegetation and soil pools to go back to predisturbance levels, highlighting the long legacy of perturbations on forest ecosystems.

Increasing the severity of individual disturbances resulted in higher peaks of nitrate export that occurred earlier in time. The simulated long-term trend in nitrate export was sensitive to the severity of individual disturbances. Several combinations of parameters could recreate a peak of nitrate export as high as the observed empirically in the 1970s during the high N period at the HBEF (∼5 kg N ha^{-1} y^{-1}) (Fig. S4*A*, green lines). However, some levels of disturbance were more likely to happen than others according to the model (Fig. S5). Best matches between model and data were obtained when tree mortality was low (<10%) for the 1906 event and moderate to high (65–85%) for the 1917 event (Fig. S5). For this subset of runs, the simulated drop in nitrate export calculated in the same way as with the empirical data ranged from 86.8 to 117 kg N ha^{-1} over the period of 1977–2007 (60–90% of the N missing). In a second scenario, we used values

of tree mortality and harvest removal as estimated in the literature (31–33) (Fig. S4, black lines). In this case, the simulated drop in nitrate export was 60.4–73.5 kg N ha^{-1} for the period 1977–2007, explaining 48.3–58.8% of the observed missing N (125 kg N ha^{-1}).

Our simulations show that the impact of past disturbances can influence N dynamics in the soil pool and concomitantly, nitrate export for many decades. Moreover, the results indicate that historical perturbations can account, at least partially, for the general pattern exhibited by nitrate losses in the HBEF, and they pose the question of how effects of present day impacts, such as climate warming, can be resolved on forest ecosystems still under the influence of past perturbations.

1. Likens GE, Buso DC, Hornbeck JW (2002) Variation in chemistry of stream water and bulk deposition across the Hubbard Brook Valley, New Hampshire, USA. *Verh Int Verein Limnol* 28:402–409.
2. Bailey AS, Hornbeck JW, Campbell JL, Eagar C (2003) *Hydrometeorological Database for Hubbard Brook Experimental Forest: 1995–2000. Technical Report NE-30* (Department of Agriculture, Forest Service Northeastern Research Station, Newtown Square, PA).
3. Buso DC, Likens GE, Eaton JS (2000) *Chemistry of Precipitation, Streamwater, and Lakewater from the Hubbard Brook Ecosystem Study: A Record of Sampling Protocols and Analytical Procedures. Technical Report NE-275* (Department of Agriculture, Forest Service Northeastern Research Station, Newtown Square, PA).
4. Winter TC, Rosenberry DO (2009) Evaluation of methods and uncertainties in the water budget. *Mirror Lake: Interactions Among Air, Land and Water*, eds Winter TC, Likens GE (Univ of California Press, Berkeley), pp 205–224.
5. LaBaugh JW, Buso DC, Likens GE (2009) Evaluations of methods and uncertainties in the chemical budget. *Mirror Lake: Interactions among air, land and water*, eds Winter TC, Likens GE (University of California Press, Berkeley, CA), pp 225–300.
6. Pettorelli N, et al. (2005) Using the satellite-derived NDVI to assess ecological responses to environmental change. *Trends Ecol Evol* 20:503–510.
7. Lindenmayer DB, Likens GE (2010) *Effective Ecological Monitoring* (CSIRO Publishing, Collingwood, VIC and Earthscan, London).
8. Whittaker RH, Bormann FH, Likens GE, Siccama TG (1974) The Hubbard Brook Ecosystem Study: Forest biomass and production. *Ecol Monogr* 44:233–254.
9. Siccama TG, et al. (2007) Population and biomass dynamics of trees in a northern hardwood forest at Hubbard Brook. *Can J Forest Res* 37:737–749.
10. Likens GE, et al. (1994) The biogeochemistry of potassium at Hubbard Brook. *Biogeochemistry* 25:61–125.
11. Helsel DR, Hirsch RM (1992) *Statistical Methods in Water Resources. Studies in Environmental Sciences 49* (Elsevier Science, Amsterdam).
12. Likens GE, Bormann FH (1995) *Biogeochemistry of a Forested Ecosystem* (Springer-Verlag, Berlin), 2nd Ed.
13. Sigman DM, et al. (2001) A bacterial method for the nitrogen isotopic analysis of nitrate in seawater and freshwater. *Anal Chem* 73:4145–4153.
14. Casciotti KL, Sigman DM, Hastings MG, Böhlke JK, Hilkert A (2002) Measurement of the oxygen isotopic composition of nitrate in seawater and freshwater using the denitrifier method. *Anal Chem* 74:4905–4912.
15. Monson RK, et al. (2006) Winter forest soil respiration controlled by climate and microbial community composition. *Nature* 439:711–714.
16. Schwartz MD, Reiter BE (2000) Changes in North American spring. *Int J Climatol* 20: 929–932.
17. Schwartz MD, Ahas R, Aasa A (2006) Onset of spring starting earlier across the Northern Hemisphere. *Global Change Biol* 12:343–351.
18. Likens GE (2000) A long-term record of ice-cover for Mirror Lake, NH: Effects of global warming? *Verh Int Ver Theor Angew Limnol* 27:2765–2769.
19. Richardson AD, Bailey AS, Denny EG, Martin CW, O'Keefe J (2006) Phenology of a northern hardwood forest canopy. *Global Change Biol* 12:1174–1188.
20. Campbell JL, et al. (2007) *Long-Term Trends from Ecosystem Research at the Hubbard Brook Experimental Forest. General Technical Report NRS-17* (US Department of Agriculture, Forest Service Northeastern Research Station, Newtown Square, PA).
21. Kaushal SS, et al. (2010) Rising stream and river temperatures in the United States. *Front Ecol Environ* 8:461–466.
22. Melillo JM, Aber JD, Muratore JF (1982) Nitrogen and lignin control of hardwood leaf litter decomposition dynamics. *Ecology* 63:621–626.
23. Finzi AC, Van Breemen N, Canham CD (1998) Canopy tree-soil interactions within temperate forests: Species effects on soil carbon and nitrogen. *Ecol Appl* 8:440–446.
24. Lovett GM, Weathers KC, Arthur MA, Schultz JC (2004) Nitrogen cycling in a northern hardwood forest: Do species matter? *Biogeochemistry* 67:289–308.
25. Templer PH, Lovett GM, Weathers KC, Findlay SE, Dawson TE (2005) Influence of tree species on forest nitrogen retention in the Catskill Mountains, New York, USA. *Ecosystems* 8:1–16.
26. Ross DS, et al. (2009) A cross-site comparison of factors influencing soil nitrification rates in northeastern USA forested watersheds. *Ecosystems* 12:158–178.
27. Ågren GI, Bosatta E (1996) *Theoretical Ecosystem Ecology: Understanding Element Cycle* (Cambridge University Press, Cambridge, UK).
28. Vitousek PM, Reiners WA (1975) Ecosystem succession and nutrient retention: A Hypothesis. *Bioscience* 25:376–381.
29. Bormann FH, Likens GE (1979) Catastrophic disturbance and the steady state in northern hardwood forest. *Am Sci* 67:660–669.
30. Goodale CL, Aber JD (2001) The long-term effects of land-use history on nitrogen cycling in northern hardwood forests. *Ecol Appl* 11:253–267.
31. Aber JD, et al. (2002) Inorganic nitrogen losses from a forested ecosystem in response to physical, chemical, biotic, and climatic perturbations. *Ecosystems* 5:648–658.
32. Peart DR, Cogbill CV, Palmiotto PA (1992) Effects of logging history and hurricane damage on canopy structure in a northern hardwoods forest. *Bull Torrey Bot Club* 119:29–38.
33. Houlton BZ, et al. (2003) Nitrogen dynamics in ice storm-damaged forest ecosystems: Implications for nitrogen limitation theory. *Ecosystems* 6:431–443.
34. Gerber S, Hedin LO, Oppenheimer M, Pacala SW, Shevliakova E (2010) Nitrogen cycling and feedbacks in a global dynamic land model. *Global Biogeochem Cycles*, 24:GB1001, 10.1029/2008GB003336.
35. Ryan DF, Bormann FH (1982) Nutrient resorption in northern hardwood forests. *Bioscience* 32:29–32.
36. Sheffield J, Goteti G, Wood EF (2006) Development of a 50-year high-resolution global dataset of meteorological forcings ate for land surface modeling. *J Climate* 19: 3088–3111.

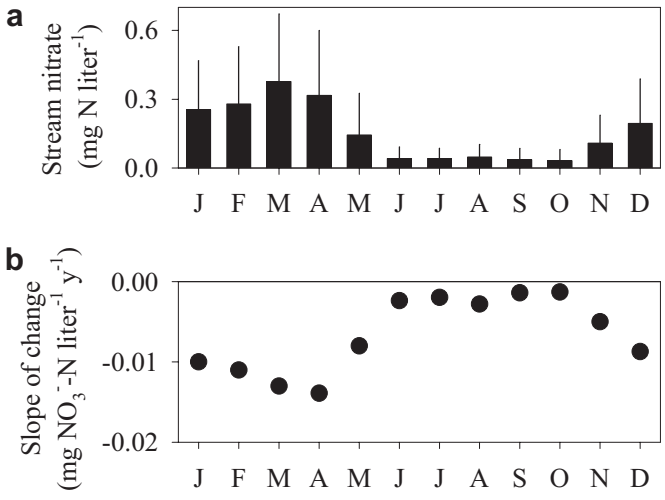

Fig. S1. Monthly VWA stream water nitrate concentration in W6 at the HBEF. (*A*) Monthly VWA stream water nitrate concentrations from 1963 to 2007 (whiskers are ±SD). (*B*) Slope of the linear fit of the long-term trend in stream water nitrate concentration by month (in all cases, $P < 0.05$). The more negative the slope, the more pronounced the nitrate decline over time.

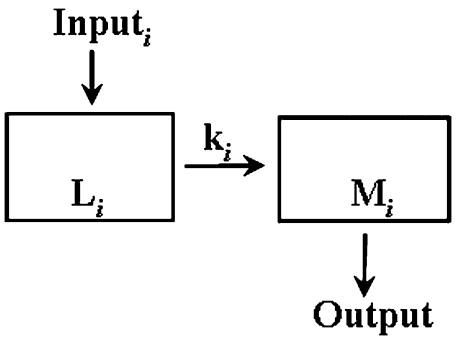

Fig. S2. Schematic representation of the applied forest floor N model. At each time step, there is an input of leaf litter to the forest floor compartment. After mineralization, nitrate is leached from the pool. *i*, respective tree species; k, mineralization rate; L, organic forest floor pool; M, available inorganic nitrogen in the forest floor pool.

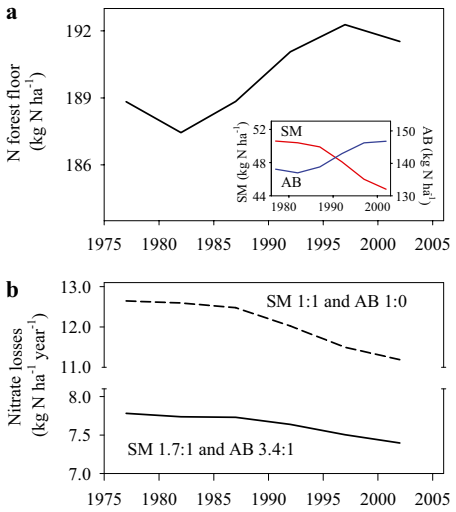

Fig. S3. Simulation of the N content in and nitrate leaching from the forest floor at the HBEF for the 1977–2002 period obtained with the forest floor N model. (*A*) Nitrogen immobilized in the forest floor over time (scenario 1). *Inset* shows the contribution from sugar maple (red line) and American beech (blue line) to the total N content. (*B*) Nitrate leached from the forest floor over time. The solid line shows simulated nitrate losses when approaching mineralized nitrate with empirical M:N rates (scenario 2). The dashed line shows nitrate losses when applying phenomenological M:N ratios (1:1 for sugar maple and 1:0 for American beech; scenario 3).

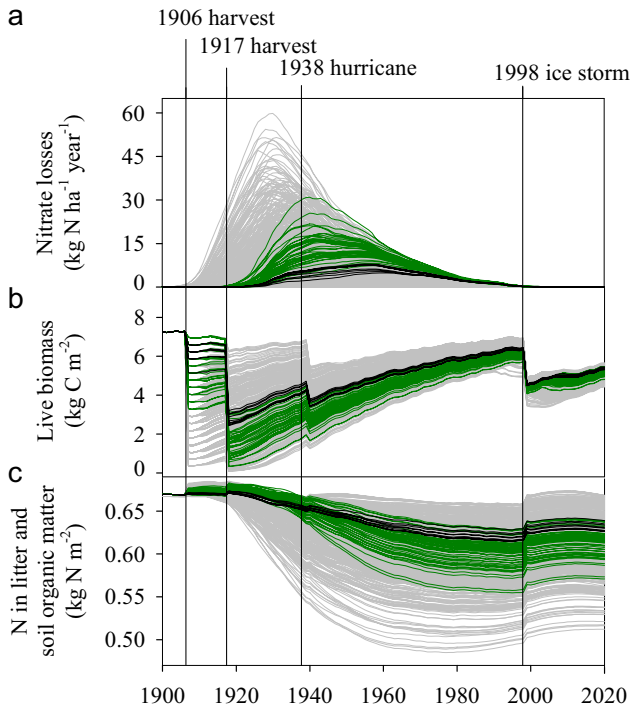

Fig. S4. Simulations of the long-term effect of historical forest perturbations on nitrate losses and the soil and vegetation pools in the HBEF obtained with the LM3V model (n = 500). The tree mortality caused by the 1938 hurricane and the 1998 ice storm was set to 20% and 30%, respectively (1, 2). The disturbance severity prescribed for the 1906 and 1917 harvest events was different in each run: tree mortality ranged from 5% to 95%, and biomass removal after harvesting ranged from 50% to 90%. Green lines represent simulations that reproduce a peak in nitrate export as observed at the HBEF in the 1970s (5.1 ± 0.4 kg N ha^{-1} y^{-1}; n = 57). Black lines denote simulations with tree mortality and harvest removal as estimated in the literature (3) (20% ± 10% and 60% ± 10% for the 1906 and 1917 harvest events, respectively; n = 9). (*A*) Stream water nitrate losses. Simulated values were smoothed using a 16-y window running average. (*B*) Carbon content in the aboveground live biomass. (*C*) Nitrogen content in the forest floor and the soil organic pool.

1. Goodale CL, Aber JD (2001) The long-term effects of land-use history on nitrogen cycling in northern hardwood forests. *Ecol Appl* 11:253–267.
2. Aber JD, et al. (2002) Inorganic nitrogen losses from a forested ecosystem in response to physical, chemical, biotic, and climatic perturbations. *Ecosystems* 5:648–658.
3. Bormann FH, Likens GE (1979) Catastrophic disturbance and the steady state in northern hardwood forest. *Am Sci* 67:660–669.

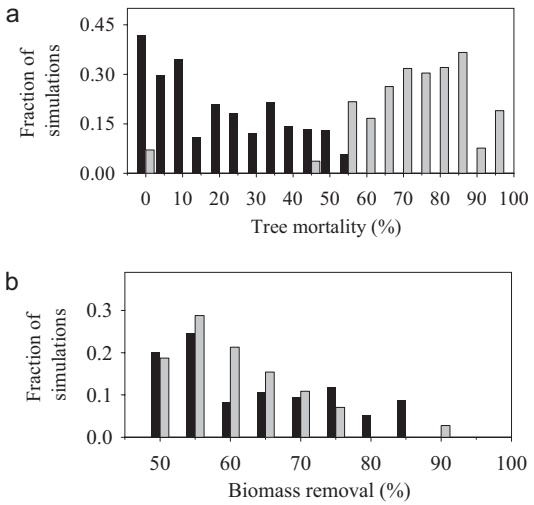

Fig. S5. Fraction of simulations that result in an export of nitrate for the 1970s similar to the export observed at the HBEF for different levels of disturbance. (*A*) Percentage of biomass killed during harvest. (*B*) Percentage of biomass removal after harvesting. Black and gray bars show the fraction of simulations for the 1906 and 1917 harvest events, respectively.

Table S1. Comparison of historic monthly average soil temperature during different periods at the HBEF

	Colman period		
Depth (cm)	1961–1966	1993–1998	SCAN period (2003–2008)
December			
8	1.6 ± 1.33*	2.65 ± 0.27*	2.28 ± 0.59*
15	2.04 ± 1.19*	3.6 ± 0.24†	3.06 ± 0.57*†
30	2.68 ± 1.23*	4.15 ± 0.36*†	4.2 ± 0.61†
January			
8	0.51 ± 0.36*	0.98 ± 0.85*†	1.08 ± 0.38†
15	1.03 ± 0.47*	1.95 ± 0.68†	1.72 ± 0.33†
30	1.42 ± 0.46*	2.27 ± 0.89*†	2.6 ± 0.35†
February			
8	0.33 ± 0.42*	0.48 ± 0.89*	0.78 ± 0.44*
15	0.66 ± 0.44*	1.61 ± 0.41†	1.32 ± 0.44†
30	1.10 ± 0.47*	1.63 ± 0.82*†	2.1 ± 0.39†
March			
8	0.31 ± 0.29*	1.06 ± 0.51†	0.8 ± 0.33†
15	0.71 ± 0.46*	1.12 ± 1.19*	1.22 ± 0.15*
30	0.86 ± 0.36*	1.53 ± 1.33†	1.88 ± 0.33†
April			
8	2.48 ± 1.82*	3.79 ± 1.73*†	4.36 ± 0.66†
15	1.9 ± 1.31*	3.18 ± 1.3*†	4.26 ± 0.61†
30	1.88 ± 0.33*	3.68 ± 1.29†	3.88 ± 0.33†

Monthly soil temperature (mean ± SD) at 8-, 15-, and 30-cm depths from December to April for the 1961–1966 and 1993–1998 periods (using Colman fiberglass sensors) and the 2003–2008 period (using encapsulated thermistors) at HBEF. For each depth, different asterisks and daggers indicate significant differences between groups ($P < 0.05$).

Table S2. Long-term trend of monthly average soil temperature at the HBEF

	Depth (cm)		
Month	8	15	30
December	+0.17* (0.34)	+0.26† (0.41)	+0.29† (0.48)
January	+0.14* (0.24)	+0.22‡ (0.35)	+0.33‡ (0.41)
February	ns	+0.23‡ (0.26)	+0.28‡ (0.34)
March	ns	+0.21‡ (0.27)	+0.32† (0.36)
April	ns	ns	ns

Goodness of the linear fit (r^2) of the long-term trend in monthly average soil temperature (8-, 15-, and 30-cm depths) from December to April for the 1961–2007 period at HBEF. The plus sign indicates increasing soil temperatures across years. The rate of increase is shown in parenthesis (°C decade^{-1}). ns, not significant.

*$P < 0.05$.

†$P < 0.001$.

‡$P < 0.01$.

Table S3. Relationship between soil temperature and stream nitrate concentration and fluxes

	Depth (cm)					
	8		15		30	
Month	NO_3-N mg L^{-1}	NO_3-N kg ha^{-1}	NO_3-N mg L^{-1}	NO_3-N kg ha^{-1}	NO_3-N mg L^{-1}	NO_3-N kg ha^{-1}
December	−0.73*	−0.63*	−0.68*	−0.62*	−0.66*	−0.61*
January	−0.41†	ns	−0.49‡	ns	−0.49‡	ns
February	ns	ns	−0.63*	−0.44†	−0.43†	ns
March	−0.50‡	−0.43†	−0.53‡	−0.42†	−0.61*	−0.49‡
April	ns	ns	ns	ns	ns	ns

Correlation coefficient (Spearman's ρ) between soil temperature (8-, 15-, and 30-cm depths) and stream nitrate concentrations (mg N L^{-1}) and between soil temperature (8-, 15-, and 30-cm depths) and stream nitrate fluxes (kg N ha^{-1}) from December to April for the 1961–2007 period at HBEF. ns, not significant.

*$P < 0.001$.

†$P < 0.05$.

‡$P < 0.01$.